

OMTN, Volume 28

Supplemental information

Directed evolution of adeno-associated virus 5 capsid enables specific liver tropism

Yuqiu Wang, Chen Yang, Hanyang Hu, Chen Chen, Mengdi Yan, Feixiang Ling, Kathy Cheng Wang, Xintao Wang, Zhe Deng, Xinyue Zhou, Feixu Zhang, Sen Lin, Zengmin Du, Kai Zhao, and Xiao Xiao

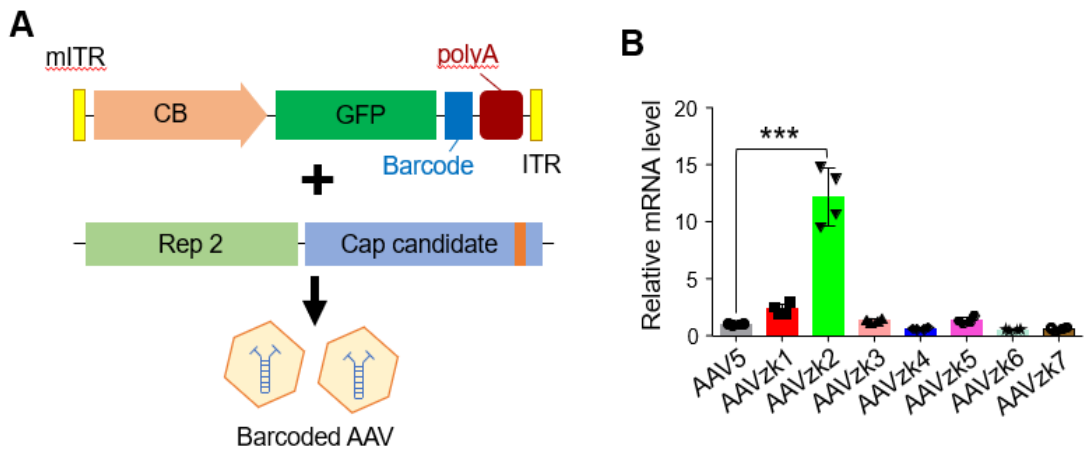


Figure S1. Screen of capsid candidate variants by barcode. (A) The scCB-GFP transgene cassette, with distinct barcode located between GFP coding sequence and bovine growth hormone (bGH) polyA signal, was encapsulated into individual capsid candidate selected from the library to produce barcoded AAV. (B) C57BL/6 mice were injected via tail vein with the barcoded AAVs at the dose of 1×10^{13} vg/kg and RT-qPCR was used to quantify barcoded GFP mRNA expression, with F primer located on the GFP coding sequence and R primer on the barcode sequence. The mRNA levels of the GFP delivered by other capsid variants were normalized to that of AAV5. *** $p < 0.001$, $n = 4$ mice (2 male, 2 female) per group. One-way ANOVA.

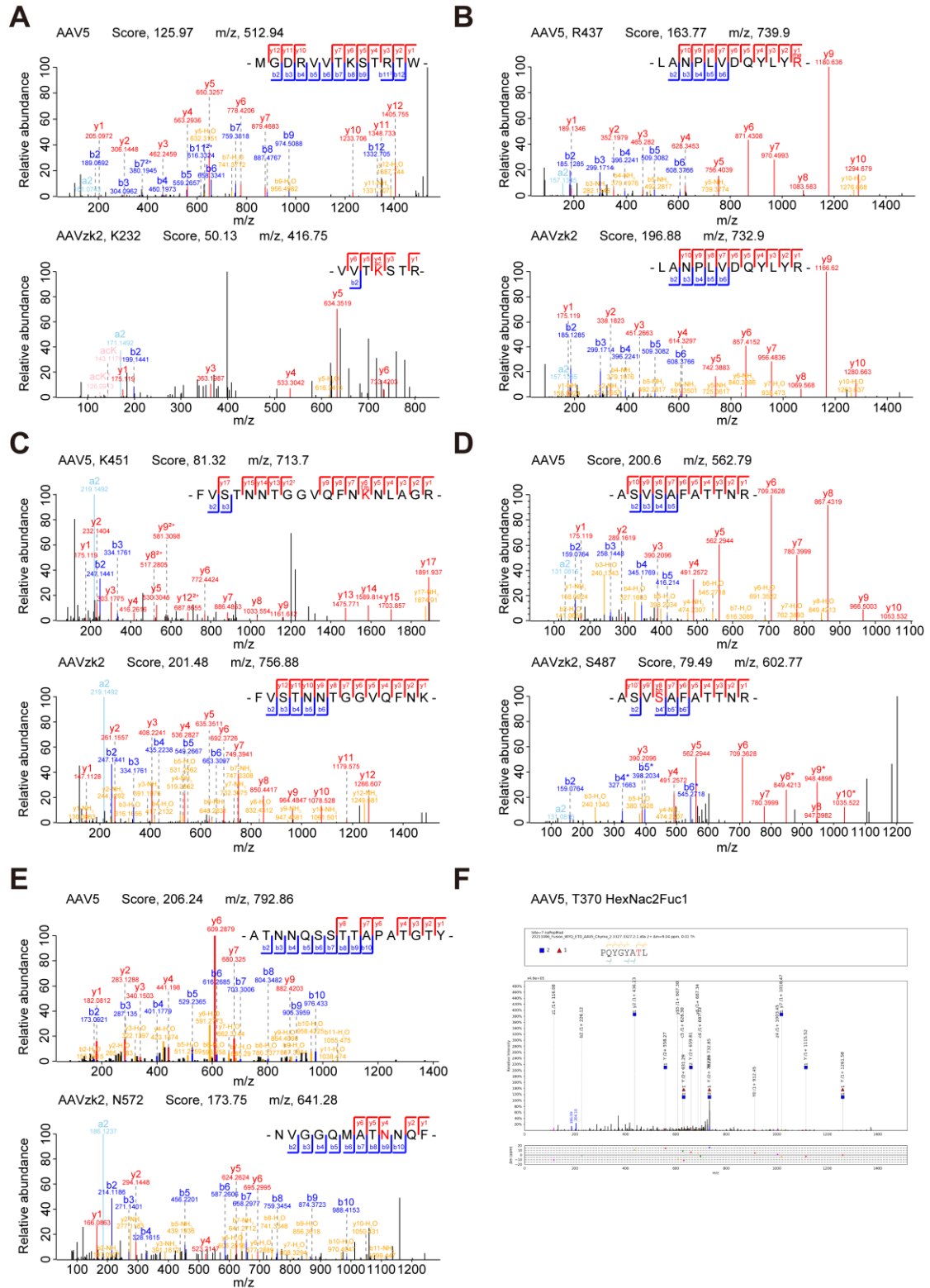


Figure S2. Representative mass spectra identified in AAV5 and AAVzk2 capsids for different PTM types. (A) Representative mass spectra for acetylation modification at AAVzk2 residue K232. (B) Representative mass spectra for methylation modification at AAV5 residue R437. (C) Representative mass spectra for ubiquitination modification at AAV5 residue K451. (D) Representative mass spectra for phosphorylation modification at AAVzk2 residue S487. (E) Representative mass spectra for deamidation

modification at AAVzk2 residue N572. (F) Representative mass spectrum for O-Glycosylation modification at AAV5 residue T370. Blue square and red triangle represented *N*-acetylhexoseamine (HexNAc) and fucose (Fuc), respectively. Mass spectra in (A-E) were analyzed using MaxQuant while mass spectrum in (F) was analyzed using pGlyco

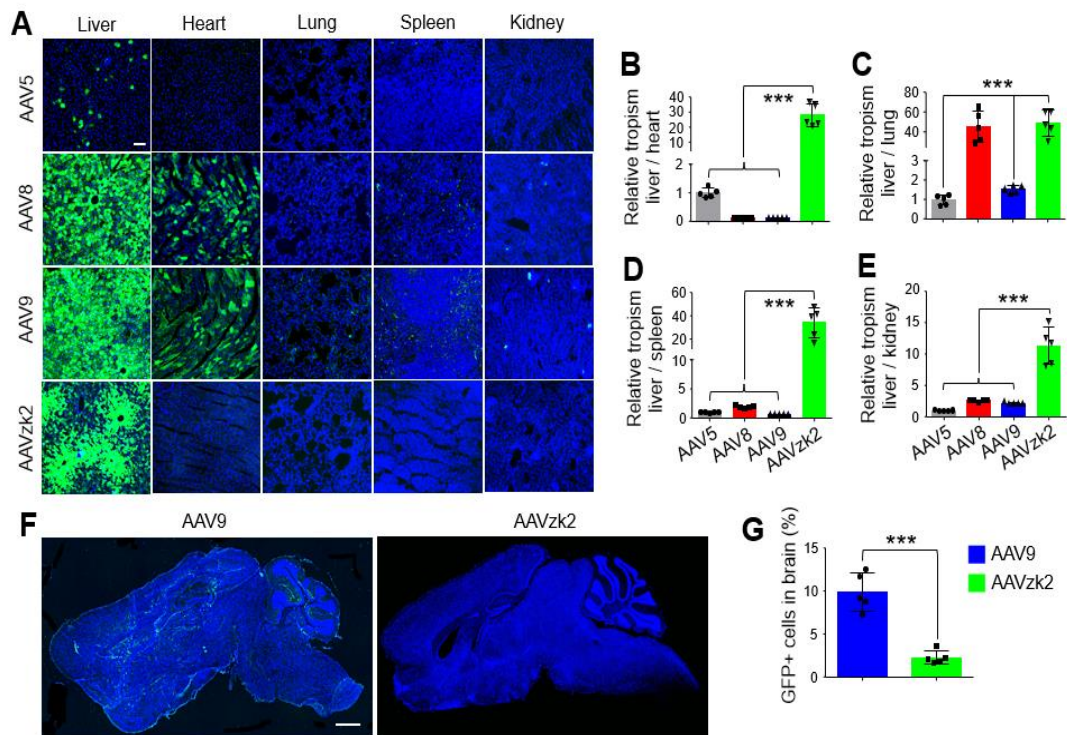


Figure S3. Preservation of superior liver specificity of AAVzk2 in female mice. (A) Female C57BL/6 mice were injected via tail vein with the indicated AAVs that carry *cis* element cassette encoding GFP at the dose of 1×10^{13} vg/kg and liver, heart, lung, spleen and kidney were stained for GFP (green) and DAPI (blue) 21 days post viral injection. Scale bar, 100 μ m. (B)-(E) Quantification of AAV tropism in liver relative to heart (B), lung (C), spleen (D) and kidney (E), which was referred to as the ratio of GFP positive liver cells versus GFP positive heart, lung, spleen and kidney cells according to DAPI spots number. $n = 5$ mice per group. *** $p < 0.001$, One-way ANOVA. (F) Female C57BL/6 mice were intravenously injected with 5×10^{13} vg/kg the indicated AAVs encoding GFP and whole brain sections were stained for GFP (green) and DAPI (blue) 3 weeks post viral injection. Scale bar, 1 mm. (G) Quantification of GFP positive cells in brain in (F), $n = 5$ mice per group. *** $p = 0.0001$, unpaired t-test.

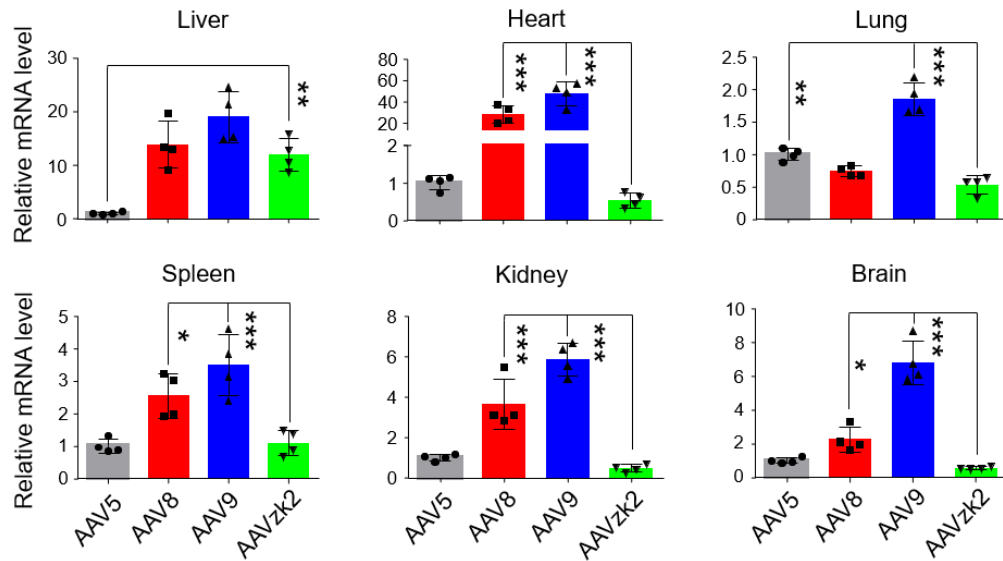


Figure S4. Relative GFP mRNA expression in female mice. Female C57BL/6 mice were injected via tail vein with the indicated AAVs that carry *cis* element cassette encoding GFP at the dose of 1×10^{13} vg/kg and liver, heart, lung, spleen, kidney and brain were subjected to RT-qPCR to detect GFP expression, in which the GFP mRNA levels in the mice treated with AAV8, 9 and zk2 were normalized to AAV5. $n = 4$ mice per group. * $p < 0.05$, ** $p < 0.01$, *** $p < 0.001$, One-way ANOVA.

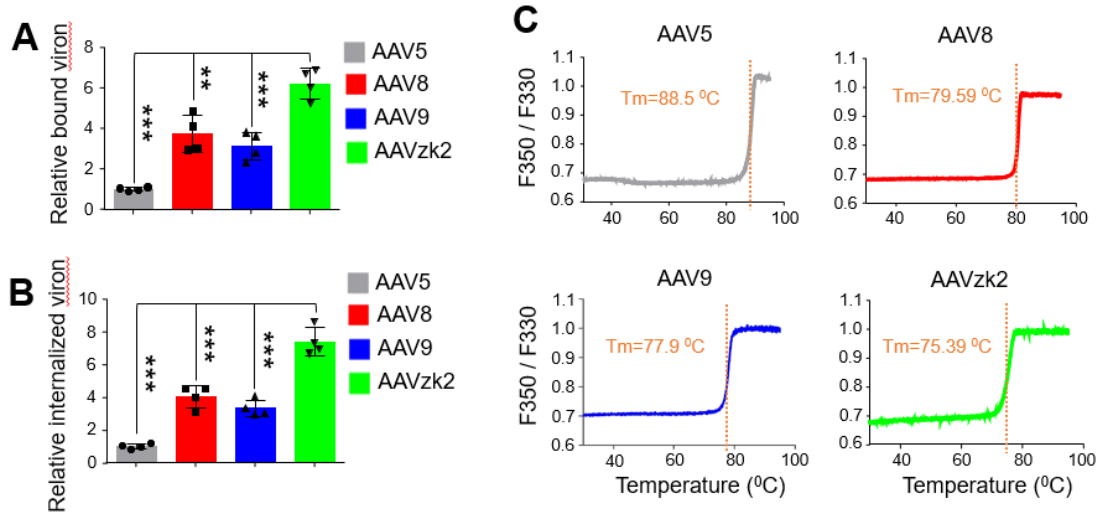


Figure S5. Distinct physicochemical and biological properties of AAVzk2 compared with AAV5. (A) Binding assay to measure the viral particles of the indicated serotypes bound to Huh7 cell surface. (B) Internalization assay to measure the internalized AAV particles by Huh7 cells. ** $p < 0.01$, *** $p < 0.001$, $n = 4$ wells of cells, One-way ANOVA. (C) AAV particles purified by iodixanol gradient ultracentrifugation were subjected to Prometheus NT. 48 platform to measure thermostability, which was determined by the ratio of fluorescence signals at 350 nm versus 330 nm (F_{350} / F_{330}) with the escalation of temperature.

Table S1. Anti-AAV neutralizing antibodies in the rhesus monkey plasma

| Monkey ID | Anti-AAV5 | Anti-AAV8 | Anti-AAV9 | Anti-AAVzk2 |
|-----------|-----------|-----------|-----------|-------------|
| 1 | 1:2 | 1:4 | 1:8 | 1:1 |
| 2 | 1:1 | 1:1 | 1:16 | 1:2 |
| 3 | 1:8 | 1:32 | 1:32 | 1:8 |
| 4 | <1:1 | 1:1 | 1:1 | 1:1 |
| 5 | <1:1 | <1:1 | <1:1 | <1:1 |
| 6 | <1:1 | <1:1 | 1:2 | <1:1 |
| 7 | 1:4 | 1:16 | 1:32 | 1:4 |
| 8 | 1:8 | 1:4 | 1:8 | 1:4 |
| 9 | 1:16 | 1:2 | 1:8 | 1:4 |
| 10 | <1:1 | 1:1 | 1:2 | <1:1 |
| 11 | 1:1 | 1:2 | 1:1 | <1:1 |
| 12 | <1:1 | <1:1 | 1:1 | <1:1 |
| 13 | 1:2 | <1:1 | <1:1 | <1:1 |
| 14 | <1:1 | <1:1 | 1:1 | <1:1 |
| 15 | <1:1 | 1:1 | 1:1 | <1:1 |
| 16 | 1:4 | 1:1 | 1:2 | 1:1 |
| 17 | 1:2 | 1:8 | 1:8 | 1:1 |
| 18 | 1:2 | 1:8 | 1:16 | 1:2 |
| 19 | 1:1 | 1:1 | 1:8 | <1:1 |
| 20 | 1:4 | <1:1 | 1:2 | <1:1 |
| 21 | 1:1 | <1:1 | 1:1 | <1:1 |

Note: The samples with neutralizing antibody titers >1:4 (Nabs positive) were marked in orange.